Two-dimensional optics with surface plasmon polaritons

Cite as: Appl. Phys. Lett. **81**, 1762 (2002); https://doi.org/10.1063/1.1506018
Submitted: 13 May 2002 . Accepted: 15 July 2002 . Published Online: 26 August 2002

H. Ditlbacher, J. R. Krenn, G. Schider, A. Leitner, and F. R. Aussenegg

Two-dimensional optics with surface plasmon polaritons

H. Ditlbacher, J. R. Krenn,[a] G. Schider, A. Leitner, and F. R. Aussenegg
Institute for Experimental Physics and Erwin Schrödinger Institute for Nanoscale Research, Karl-Franzens-University Graz, A-8010 Graz, Austria

(Received 13 May 2002; accepted for publication 15 July 2002)

We report the experimental realization of highly efficient optical elements built up from metal nanostructures to manipulate surface plasmon polaritons propagating along a silver/polymer interface. Mirrors, beamsplitters, and interferometers produced by electron-beam lithography are investigated. The plasmon fields are imaged by detecting the fluorescence of molecules dispersed in the polymer. © *2002 American Institute of Physics.* [DOI: 10.1063/1.1506018]

The downsizing of photonic devices towards nanoscale dimensions meets two major difficulties. First, as a fundamental limitation diffraction restricts the minimum lateral dimensions of dielectric optical elements and waveguides to about half the effective light wavelength. Second, the light fields in conventional optics are essentially three-dimensional, rendering the realization of highly integrated planar devices rather complicated from a technological point of view. Recent results demonstrate that optics based on surface plasmon polaritons (SPPs) allows us to overcome the first limitation.[1] In this letter, we show that SPPs are suited as well to realize a two-dimensional counterpart of conventional optics.

SPPs are electromagnetic modes constituted by a light field coupled to a collective electron oscillation propagating along an interface between a metal and a dielectric. As SPPs are surface waves, their field intensity is maximum in the interface and decays exponentially along the directions perpendicular to it. The SPP field strength in the interface is strongly enhanced with respect to the exciting optical field. Although the ohmic damping of SPPs is rather strong, $1/e$ propagation lengths of a few tens of μm are reported for SPPs excited with visible light on silver or gold.[2] This value seems sufficiently large for highly integrated optical devices with correspondingly short signal paths.

The strong confinement of SPP fields at a metal/dielectric interface indicates the feasibility of a SPP-based quasi-two-dimensional optics. Recent contributions to this topic include theoretical simulations as the investigation of SPP scattering and reflection by surface defects.[3–7] Experimentally, SPP propagation along flat thin metal films[8] and μm wide metal stripes was investigated.[9] The influence of surface defects on SPP propagation was probed with near-field optical microscopy[10–13] and first proposals for SPP optical elements corresponding to their conventional counterparts like lenses or mirrors were made.[14] Furthermore, experiments on SPP photonic band-gap structures were reported.[15,16] However, when it came to the investigation of SPP optical elements constituted by surface defects, the experimental results indicated a rather weak interaction of SPPs with the elements, probably due to poor experimental control of the defect geometry. In contrast, we present here a highly efficient SPP mirror and a 50/50 SPP beamsplitter. Finally, we combine these elements to a SPP interferometer.

We investigate SPPs propagating along the surface of a silver thin film deposited on a glass substrate. The SPP optical elements are constituted by nanoscale surface structures, as depicted in Fig. 1. These structures are produced by standard electron-beam lithography (EBL).[17] First, the optical element geometry is transferred to a 100-nm-thick polymethyl–metacrylate (PMMA) film on a glass substrate by exposure to the electron beam of a scanning electron microscope. After chemical development of the PMMA mask, 70 nm of SiO_2 are deposited onto the sample by electron-beam-assisted evaporation. After lift-off of the PMMA mask, the SiO_2 structures remain on the glass substrate. In a last step, the whole sample area is coated by a 70-nm-thick silver film by thermal evaporation. We thus end up with surface structures constituted by 70-nm-high height modulations of the 70-nm-thick silver film. In the following we refer to these height modulations as *particles* or *wires* depending on the geometry of the SiO_2 structures defining the respective modulation.

SPPs are launched locally by focusing a laser beam (Ti:sapphire, $\lambda_0 = 750$ nm, power 5 mW) through a microscope objective (50×, numerical aperture 0.85) perpendicularly to the substrate plane on an EBL-produced nanowire[18] (see Fig. 1). To visualize the spatial SPP field distribution we apply fluorescence imaging, as reported in Ref. 14. This

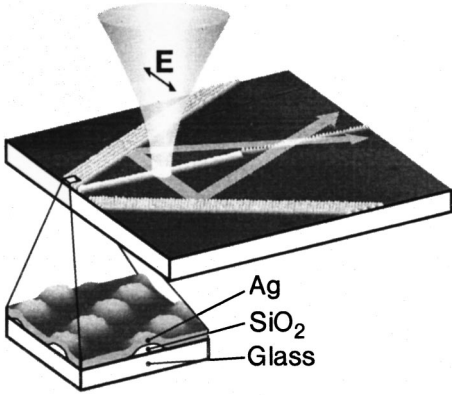

FIG. 1. Experimental setup: sketch of the nanoscale surface structures combined with an atomic force microscope image of the sample surface. The double arrow indicates the polarization direction of the incident light.

[a]Electronic mail: joachim.krenn@kfunigraz.ac.at

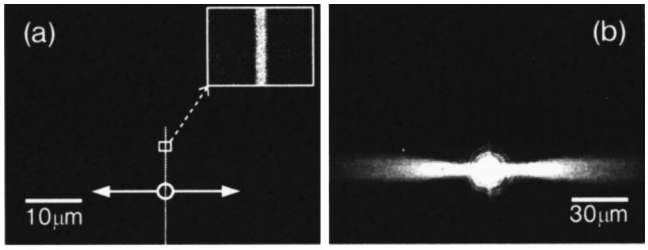

FIG. 2. (a) Scanning electron micrograph (SEM) of the nanowire (width 160 nm, height 70 nm, length 20 μm) for SPP launch; the inset shows a 12× magnified image of the area marked by the white box. The circle defines the focus position and the arrows indicate the direction of SPP propagation; (b) corresponding fluorescence image.

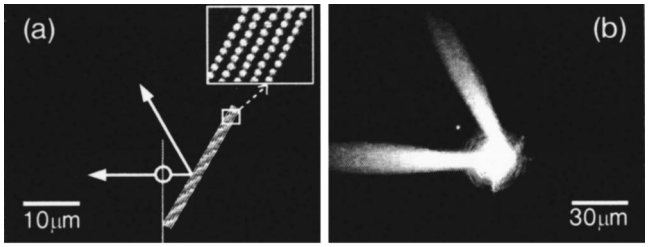

FIG. 3. (a) SEM of the SPP Bragg reflector built up from individual nanoparticles (diameter 140 nm, height 70 nm); the inset shows a 7× magnified image of the area marked by the white box. The circle defines the focus position and the arrows indicate the direction of SPP propagation; (b) corresponding fluorescence image.

technique relies on the fluorescence of molecules placed in the vicinity of the SPP-carrying metal/dielectric interface. In contrast to previous work where SPPs excited at $\lambda_0 = 515$ nm were probed by Rhodamin 6G molecules, we use $\lambda_0 = 750$ nm for the present work as SPP damping in the red spectral range is strongly decreased and, therefore, the SPP propagation length increases.[2] With an absorption maximum at a wavelength of $\approx$750 nm and sufficient chemical stability, we use 1,1′-dipropyl-3,3,3′,3′-tetramethylindotricarbocyanine iodide (DiR, Lambda Fluorescence Technology, Kirchbach, Austria) as the fluorescence probe. A 10^{-4} molar solution of DiR is prepared by dispersing the molecules in a solution of 1% PMMA in chlorobenzene. The resulting solution is spin cast on the samples yielding a uniform film 30 nm thick when dried. Compared to the previously reported method of depositing the molecules by vacuum sublimation atop a SiO_2 spacer layer, this technique requires only one handling step of the sample. By angle-resolved reflectivity in an attenuated total reflection setup,[19] we determined the SPP wavelength to be $\lambda_{pl} = 610$ nm for $\lambda_0 = 750$ nm and the used PMMA film thickness of 30 nm. The 1/*e* propagation length is estimated to be in the order of 10 μm. The presence of the DiR molecules at the used concentration leads to a negligible SPP damping as compared to an undoped PMMA film. The fluorescence images are acquired through the microscope objective used for SPP excitation and an edge filter (cutoff wavelength, 790 nm) by a high-sensitivity charge-coupled-device camera.[18]

In the following, we demonstrate the step-by-step realization of a SPP interferometer by adding one optical element each step. The figures show the respective scanning electron micrographs and fluorescence images. We note that the corresponding images are displayed on different scales as indicated by the length bars. In the fluorescence images the gray levels in the area close to the SPP launch site are saturated to improve the visualization of SPP propagation. We start with the local excitation of two counterpropagating directed SPPs by focusing the laser beam on a nanowire 160 nm wide and 20 μm long, as seen in the two scanning electron micrographs in Fig. 2(a). The fluorescence image in Fig. 2(b) reveals two highly directed SPPs with a divergence angle mainly determinded by the laser focus diameter.[18]

Next, we aim at realizing a SPP mirror. Theoretical considerations show that *individual* protuberances or indentations in the metal film lead to rather low reflection coefficients for an incident SPP.[6] Therefore, we use an *ensemble* of nanoparticles (diameter 140 nm) arranged in parallel lines to act as a Bragg reflector.[15,16] Setting the incidence angle of the SPP to 60° with regard to the particle line direction requires a distance between the lines of 350 nm to fulfill the Bragg condition to first order [Fig. 3(a)]. The distance between the nanoparticles within a line is set to 220 nm. As found experimentally, five particle lines are sufficient for a deflection of the incident SPP with high efficiency. This is clearly seen in Fig. 3(b), where the SPP propagating to the right is deflected with low loss in intensity and directionality. From Fig. 3(b), the reflection coefficient is estimated to about 90%. As the transmitted SPP intensity is found to be negligible, this result implies that roughly 10% of the incident SPP intensity are scattered to light. Further experiments (not shown here for the sake of brevity) with different sample geometries and/or light wavelengths prove that the observed SPP deflection is indeed due to Bragg scattering.

As displayed in Fig. 4(a), we now add a linear row of nanoparticles (diameter 140 nm) to act as a beamsplitter on the SPP deflected by the mirror. The interparticle distance was set to 280 nm, for which a ratio of the reflected and transmitted SPP intensities of unity was found. Again, the quantitative analysis of the SPP intensities before and after passing the beamsplitter shows that SPP scattering to light is rather low.

Finally, we complete the SPP interferometer by adding a second mirror that deflects the SPP propagating to the left, see Fig. 1 and the inset in Fig. 5. Now, both SPPs launched from the nanowire are deflected and impinge on the beamsplitter. We produced a series of such interferometers with varying horizontal positions of the right SPP mirror, as indi-

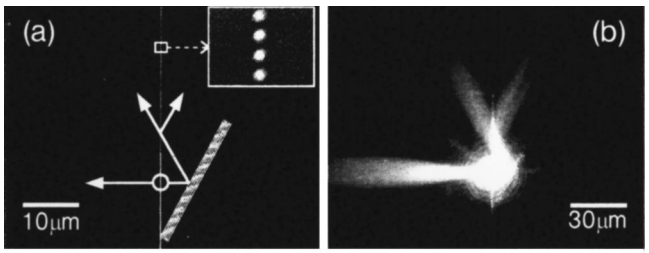

FIG. 4. (a) SEM of the SPP beamsplitter built up from individual nanoparticles (diameter 140 nm, height 70 nm); the inset shows a 12× magnified image of the area marked by the white box. The circle defines the focus position and the arrows indicate the direction of SPP propagation; (b) corresponding fluorescence image.

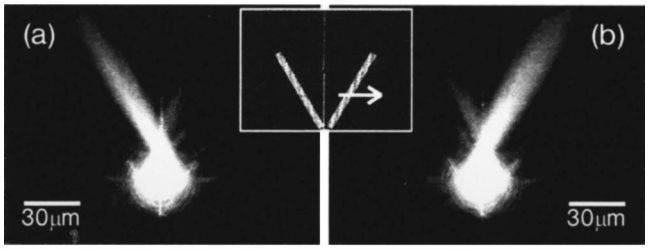

FIG. 5. (a) SPP interferometer: The arrow in the SEM (inset) indicates the lateral position change of the right SPP mirror between the images (a) and (b), which show the corresponding fluorescence images.

cated by the arrow in the inset in Fig. 5. The corresponding fluorescence images reveal that the SPP intensities within the two exits of the interferometer vary as a function of the lateral mirror position, switching from one exit to the other. Two examples are reported in Figs. 5(a) and 5(b). The relative difference of the lateral mirror positions for these two interferometers yields an average difference of 300 nm for the SPP propagation lengths between the SPP launch site and the beamsplitter. This value corresponds to $\lambda_{pl}/2=305$ nm. As we see in the fluorescence images in Figs. 5(a) and 5(b), the integral SPP intensity after passing the beamsplitter is found to be maximum either in the left or in the right exit [compare, also, Fig. 3(b),] as would be expected for a conventional interferometer. This finding indicates that there is a difference in phase shift of the SPPs transmitted and reflected by the beamsplitter, as in the case of a conventional interferometer. For a more elaborate investigation of the SPP interaction with the respective optical elements a study with near-field optical microscopy with correspondingly high spatial resolution is desirable.

In summary, we have developed and tested microscale SPP mirrors, beamsplitters, and interferometers. Due to the high sensitivity of interferometric measurements, the latter seems especially appealing for optical sensor and monitoring applications, as, e.g., small changes in the effective refractive index within one interferometer arm could be detected. In principle, SPP optical elements allow us to realize a variety of two-dimensional optical circuits. Such circuits could lead to the technologically easy and cost effective realization of all-optical switches, integrated photonic devices, and optical lab-on-a-chip applications. Moreover, the miniaturization of SPP optical elements is not hindered by the diffraction limit, rendering the realization of nanoscale photonic devices possible.

For financial support, the Austrian Ministry for Technology and the Austrian Science Foundation, Grant No. P14292, are acknowledged.

[1] J. R. Krenn, J. C. Weeber, A. Dereux, E. Bourillot, J. P. Goudonnet, G. Schider, A. Leitner, F. R. Aussenegg, and C. Girard, Phys. Rev. B **60**, 5029 (1999).
[2] B. Lamprecht, J. R. Krenn, G. Schider, H. Ditlbacher, M. Salerno, N. Felidj, A. Leitner, F. R. Aussenegg, and J. C. Weeber, Appl. Phys. Lett. **79**, 51 (2001).
[3] F. Pincemin, A. A. Maradudin, A. D. Boardman, and J. J. Greffet, Phys. Rev. B **50**, 15261 (1994).
[4] F. Pincemin and J. J. Greffet, J. Opt. Soc. Am. B **13**, 1499 (1996).
[5] J. A. Sanchez-Gil, Phys. Rev. B **53**, 10317 (1996).
[6] J. A. Sanchez-Gil, Appl. Phys. Lett. **73**, 3509 (1998).
[7] U. Schröter and D. Heitmann, Phys. Rev. B **58**, 15419 (1998).
[8] P. Dawson, F. de Fornel, and J. P. Goudonnet, Phys. Rev. Lett. **72**, 2927 (1994).
[9] J. C. Weeber, J. R. Krenn, A. Dereux, B. Lamprecht, Y. Lacroute, and J. P. Goudonnet, Phys. Rev. B **64**, 045411 (2001).
[10] I. I. Smolyaninov, D. L. Mazzoni, and C. C. Davis, Phys. Rev. Lett. **77**, 3877 (1996).
[11] J. R. Krenn, R. Wolf, A. Leitner, and F. R. Aussenegg, Opt. Commun. **137**, 46 (1997).
[12] S. I. Bozhevolnyi and F. A. Pudonin, Phys. Rev. Lett. **78**, 2823 (1997).
[13] S. I. Bozhevolnyi and V. Coello, Phys. Rev. B **58**, 10899 (1998).
[14] I. I. Smolyaninov, D. L. Mazzoni, J. Mait, and C. C. Davi, Phys. Rev. B **56**, 1601 (1997).
[15] W. L. Barnes, T. W. Preist, S. C. Kitson, and J. R. Sambles, Phys. Rev. B **54**, 6227 (1996).
[16] S. I. Bozhevolnyi, J. E. Erland, K. Leosson, P. M. W. Skovgaard, and J. M. Hvam, Phys. Rev. Lett. **86**, 3008 (2001).
[17] M. A. McCord and M. J. Rooks, in *Handbook of Microlithography, Micromachining, and Microfabrication*, edited by P. Rai-Choudhury (SPIE and The Institution of Electrical Engineers, Bellingham, Washington, 1997), Vol. 1, Chap. 2, pp. 139–249.
[18] H. Ditlbacher, J. R. Krenn, N. Felidj, B. Lamprecht, G. Schider, M. Salerno, A. Leitner, and F. R. Aussenegg, Appl. Phys. Lett. **80**, 404 (2002).
[19] H. Raether, in *Surface Plasmons, Springer Tracts in Modern Physics*, edited by G. Höhler (Springer, Berlin, 1988), Vol. 111.